Textural entropy as a potential feature for quantitative assessment of jaw bone healing process

Michał Kołaciński[1], Marcin Kozakiewicz[1], Andrzej Materka[2]

[1]Department of Maxillofacial Surgery, Medical University of Lodz, Lodz, Poland
[2]Medical Electronics Division, Technical University of Lodz, Lodz, Poland

Submitted: 25 August 2012
Accepted: 18 November 2012

Arch Med Sci
DOI: 10.5114/aoms.2013.33557

Corresponding author:
Michał Kołaciński MD, DDS
Department of Maxillofacial Surgery, Medical University of Lodz
113 Żeromskiego Str.
90-549 Lodz, Poland
Phone: +48 42 6393781
E-mail: mkolacinski@wp.pl

Abstract

Material and methods: One hundred and twenty radiographs with loss of bone architecture were investigated (a bone defect was circumscribed - ROI DEF). A reference region (ROI REF) of the same surface area as the ROI DEF was placed in a field distant from the defect, where a normal, trabecular pattern of bone structure was well visualized. Data of three time points were investigated: T0 – immediately after the surgical procedure, T1 – 3 months post-op, and T2 – 12 months post-op.

Results: Textural entropy as a parameter describing bone structure regeneration was selected based on Fisher coefficient (*F*) evaluation. *F* was highest in T0 (3.4) and was decreasing later in T1 (1.7) and T2 (1.0 – means final lack of difference in the structure to reference bone). Textural entropy is a measure of structure disarrangement which in a bone defect region attains minimal value due to structural homogeneity, i.e. low complexity of the texture. The calculated parameter in the investigated material revealed a gradual increase inside the bone defect ($p < 0.05$), i.e. increase of complexity in a time-dependent manner starting from immediate post-op (T0 = 2.51; T1 = 2.68) up to most complex 1 year post-operational (T2 = 2.73), reaching the reference level of a normal bone.

Conclusions: Textural entropy may be useful for computer assisted evaluation of bone regeneration process. The complexity of the texture corresponds to mature trabecular bone formation.

Key words: textural entropy, bone healing, digital radiograph.

Introduction

Bone tissue regeneration means substitution of blood clot with connective tissue and finally with new bone formation. The molecular physiology of bone metabolism plays a key role in the understanding of bone disorders [1]. Bone formation can be indirectly assessed by measuring serum agents, for example osteocalcin [2]. Yet the dynamic process in bone tissue structure can be followed either with histomorphometric or radiological analysis [3]. Morphological changes of bone tissue (remodeling) visualized on radiographs can be useful for assessment of surgery results [4]. In oral surgery and periodontology intra-oral plain radiograph is still the least affecting radiological examination for a patient. It is widely used in follow-up studies due to its accessibility and simplicity [5-7].

In this study the authors would like to present a method of objective radiograph assessment based on computer analysis. The main difficulty encountered in the literature is setting a comparable feature for computer processing. Parameters related to the fractal dimension and co-occurrence run-length matrix have been used in osteoporosis studies, but there is still no single feature useful for oral surgery [8, 9]. Most parameters proposed to describe microstructure of bone tissue in radiographic examination require removal of post-processing artifacts [10].

The aim of the study is to present textural entropy as a potential parameter to quantitatively assess the jaw bone healing process using two-dimensional radiographic examination.

Material and methods

Intraoral, standardized, digital radiographs were taken into consideration (clinical images included from the archive of the Department of Maxillofacial Surgery; the radiographs were taken during typical clinical follow-up, Ethical Board permission: RNN/485/11/KB). The Digora Optime system of digital radiography (Soredex, Tuusula, Finland) was applied in this study. Radiographs were taken in a standardized way. We applied a modified RINN system, from which we utilized the ring (with clicks for RINN positioner) and film plate holder (vertical and horizontal). The ring was placed on an X-ray camera tube and a film plate holder was fixed with a connecting bar bent at the right angle. The ring in the camera was joined by an additional adapting ring that was rigidly fixed to the X-ray tube. We applied an enveloped storage phosphor plate to facilitate analog to digital conversion without any chemical film processing. A bite index was prepared using a silicone material (occlusal bite duplicates the shape of the film plate holder and the occlusal surfaces of the teeth). The X-ray detector was placed in the RINN positioner and the bite index with the connection bar and the ring was placed in the patient's mouth and fixed to the tube. The same radiological equipment was used: Focus X-ray intraoral unit (Instrumentarium Dental, Tuusula, Finland). Technical parameters of exposure were the same in all included radiographs: 7 mA, 70 mV and 0.1 s. Image size: 476 × 620 pixels. Pixel size was 70 µm × 70 µm. Final radiographs were 8 bits/pixel (min. lum.: 1; max. lum.: 255).

Radiographs with the loss of bone architecture in maxilla or mandible after surgical procedures of apicoectomy were included in the study. Apicoectomy (root end surgery) is a commonly performed dental root tip removal procedure, necessitated when conventional root canal therapy has failed. Radiographs were grouped depending on gender (males and females) and location of the bone defect (maxilla or mandible). Furthermore, every group was divided into subgroups depending on the healing time (i.e. duration of the post-operational period): directly after the procedure (T0), 3 months after the procedure (T1) and 12 months after the surgical procedure (T2). It was assumed that directly after the procedure (T0) bone healing does not take place while after 12 months (T2) the healing process is completed. Group T1 should demonstrate intermediate feature values between groups T0 and T2. For statistical needs the 10 best quality radiographs were included in each group (i.e. the groups were equal). Two researchers qualified the radiographs independently. They were chosen on the basis of visual inspection. Only radiographs of sufficient quality accepted by both inspectors independently were included in the study. Initially, radiograph samples with the most typical bone trabeculation were found for reference group construction (REF), then radiographs of post-apicoectomy bone defects were included (T0) and later images with signs of bone healing (T1) and finally images of the totally healed area (T2). The total number of radiographs included was 120.

The bone defect (or hereinafter also bone regeneration region) visualized in the radiograph was circumscribed within its internal border (ROI DEF). The reference region (ROI REF) was defined, of the same area as the ROI DEF but in a field distant from the defect, where the normal trabecular pattern of bone structure was well visualized. The average region of interest (ROI) size was 2519 pixels. A model series of the analyzed radiographs is shown in Figure 1. The images were analyzed using MaZda ver. 4.5 computer software developed by Technical University of Lodz programmers [11]. The images were normalized to share the same mean and standard deviation inside ROIs ("$\mu \pm 3\sigma$" MaZda option, where μ and σ denote the mean and standard deviation of registered optical density, respectively). Selection of the feature was done based on the value of Fisher coefficient (F) to describe the difference between the ROI in bone defect versus the ROI of reference bone: $F = D/V$, where D denotes between-ROI scatter, V denotes within-ROI variance.

The interpretation of the Fisher coefficient is as follows: any value above 1.0 indicates a significant difference between ROI REF and investigated ROI (T0, T1, T2) – the higher the F value, the bigger the difference between ROIs; any values of 1.0 and less describe the no-difference region in the radiograph [12].

The second-order histogram was defined as the co-occurrence matrix $h_{d\theta}(i,j)$. When divided by the total number of neighboring pixels $R(d,\theta)$ in ROI, this matrix becomes the estimate of the joint prob-

Figure 1. Series of analyzed radiographs. T0 – bone defect. T1 – new bone formation. T2 – matured bone. Regions of interest were located in areas typical for bone regeneration – the green region marks the reference bone, the red region marks the bone defect site

ability, $p_{d\theta}(i,j)$, of two pixels, a distance d apart along a given direction θ, having particular (co-occurring) values i and j of optical density. Formally, given the image $f(x,y)$ with a set of 256 discrete grey levels (N), the matrix $h_{d\theta}(i,j)$ is defined such that its $(i,j)_{th}$ entry is equal to the number of times that:

$f(x_1,y_1) = i$ and $f(x_2,y_2) = j$, where $(x_2,y_2) = (x_1,y_1) + (d \cos \theta, d \sin \theta)$.

This yields a square matrix of dimension equal to the number of grey levels in the radiograph, for each distance d and orientation θ. The distances $d = 5$ pixels (equal to the minimum thickness of jaw bone trabeculae in our study) with angles $\theta = 0°$, 45°, 90° and 135° (functionality provided by the software) were considered in this study to find more information included in the radiograph. Next, entropy values computed for the 4 directions were averaged to reduce the feature dependence on image rotation. Due to that, the observed entropy in the radiograph presented local texture in a more precise manner.

The following well-known formula was used to describe the entropy of the ROI texture:

$\text{entropy} = -\Sigma_{i=1}^{N_{255}} \Sigma_{i=1}^{N_{255}} p(i,j) \log (p(i,j))$, where Σ is sum, N is the number of levels of optical density in the radiograph, i and j are optical density of pixels 5-image-point distant one from another, p is probability, log is logarithm.

Statistical analysis

T-test (to compare time-dependent alterations) and ANOVA (to check the influence of location or gender on parameter variability) were applied for statistical analysis, and $p < 0.05$ was assumed as the significance level. Assessment of standardized skewness and standardized kurtosis was the basis to confirm normal distribution of the data (Statgraphics Centurion XVI, StatPoint Technologies. Inc., Virginia, USA).

Results

Analyzing entropy, ROI DEF versus ROI REF was calculated as the ratio of between-ROI scatter to within-ROI variance. That ratio described a high difference between the ROI DEF and the ROI REF at T0, which decreased later at T1 and T2: 3.4, 1.7, and 1.0, respectively. The value of 1.0 indicates a lack of any differences between the investigated ROIs.

The reference bone was characterized radiographically by the proposed entropy as relatively high-value texture (2.76 ±0.18). Entropy of the bone defect was significantly ($p < 0.05$) lower at T0 (2.51 ±0.24; $t = -5.3121$; $p < 0.00001$) than in the reference bone, T1 samples (2.68 ±0.18; $t = 3.5786$; $p < 0.001$) and T2 (2.73 ±0.18; $t = 4.5687$; $p < 0.00001$). At T1 it was only lower than in REF ($t = -2.0675$; $p < 0.05$). In the last investigated period (T2), the bone structure in the operation site was similar to the reference and T1, and entropy was significantly higher than at T0 ($t = -4.5687$; $p < 0.05$).

The entropy of bone defect radiographs in males and females was equally low, contrary to the reference or the healed bone, where it was of a high value. The mean value of the evaluated parameter was significantly decreased in the bone defect versus the reference bone – especially in male samples. Then, during the bone healing, the entropy increased toward the reference value (quicker in males). The bone defect during the healing (T1 vs. REF) became more similar to a normal bone (Table I).

ANOVA revealed that the jaw bone defect healing had the same pattern regardless of gender ($p = 0.46$ for T0, $p = 0.1$ for T1 and $p = 0.33$ for T2; $p = 0.4$ for REF). Comparison of gender-dependent entropy distribution in bone defect during the process of healing is shown in Figure 2. The same parameters for the defect location factor revealed that jaw bone healing pattern is independent from the defect location too ($p = 0.86$ for T0, $p = 0.26$ for

Table I. Entropy according to gender and time of healing

	N	Average	Median	Standard deviation	Minimum	Maximum	Range	Standard skewness	Standard kurtosis
T0_F_DEF	20	2.54	2.59	0.23	2.02	2.82	0.81	–1.38	–0.16
T1_F_DEF	20	2.63	2.63	0.17	2.3	2.91	0.62	–0.31	–0.48
T2_F_DEF	20	2.75	2.77	0.14	2.42	2.97	0.55	–1.68	0.59
T0_M_DEF	20	2.48	2.53	0.26	2.05	2.88	0.83	–0.55	–1.01
T1_M_DEF	20	2.73	2.8	0.18	2.29	2.94	0.65	–1.69	0.22
T2_M_DEF	20	2.7	2.73	0.18	2.38	3.02	0.64	–0.53	–0.47
M_REF	20	2.79	2.83	0.2	2.43	3.05	0.61	–0.61	–1.12
F_REF	20	2.74	2.75	0.15	2.43	2.97	0.54	–0.75	–0.35

n – number of cases, T0 – immediately after surgery, T1 – 3 months post-operationally, T2 – 12 months post-operationally, F – female, M – male, DEF – bone defect, REF – reference bone

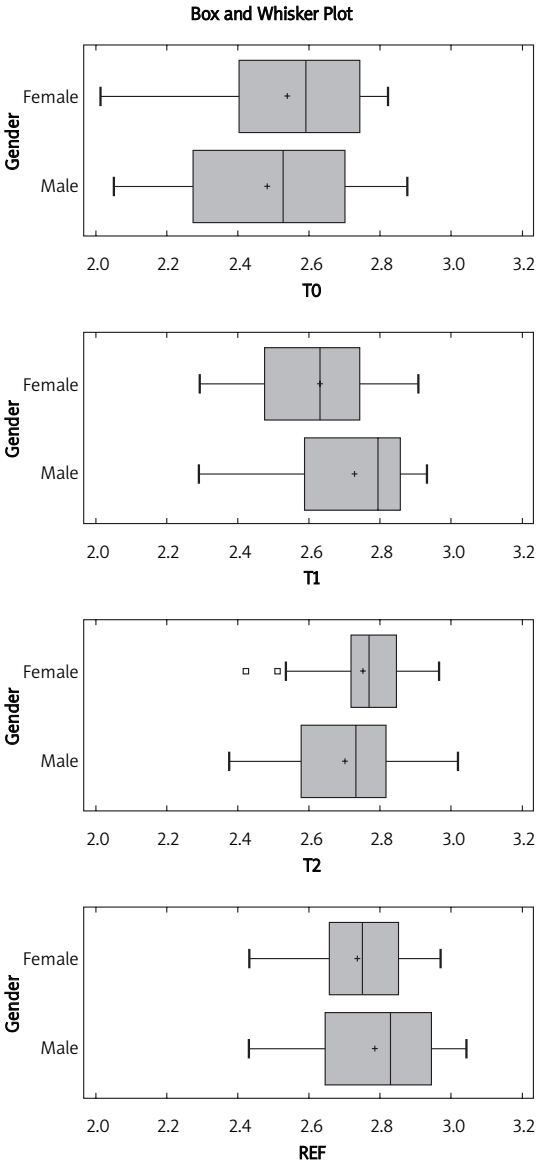

Figure 2. Comparison of gender-dependent entropy distribution in bone defect during the process of healing
T0 – immediately after surgery, T1 – 3 months post-operationally, T2 – 12 months post-operationally

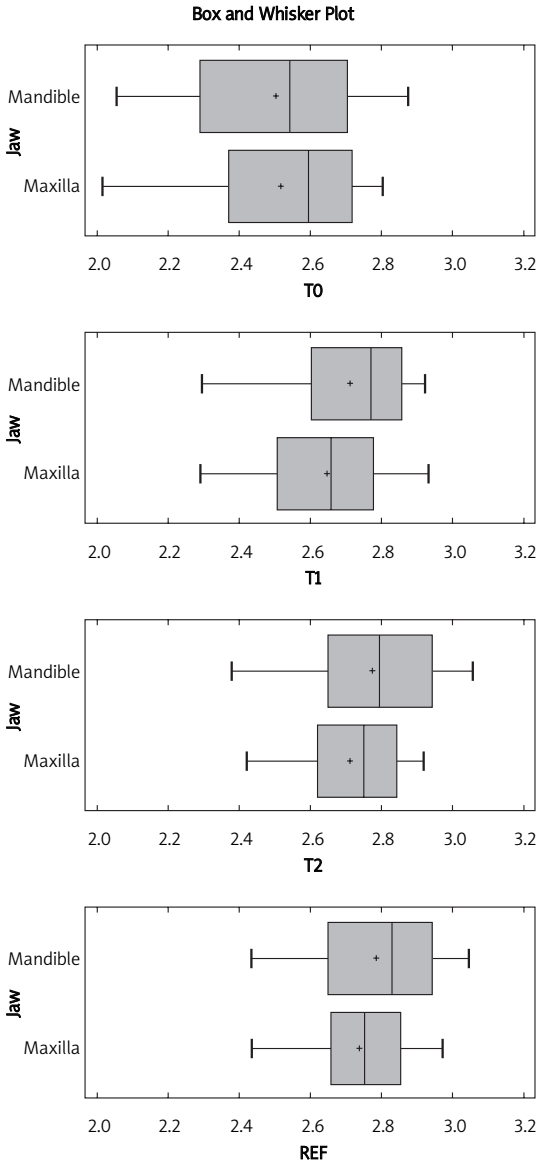

Figure 3. Comparison of location dependent entropy distribution in bone defect during the process of healing

T1 and $p = 0.31$ for T2; $p = 0.4$ for REF). This means that the jaw bone healing pattern is the same in maxilla and mandible, regardless of the time of healing. Comparison of location-dependent entropy distribution in bone defect during the process of healing is shown in Figure 3. Summary statistics of texture parameter entropy are shown in Table II.

Discussion

Morphological X-ray assessment plays a key role in describing pathology and regeneration of hard tissue. This paper focuses on characterization of the bone healing process combined with its structural analysis. It is a quantitative method based on objective computer analysis of low-dose intra-oral radiographs which requires definition of comparable parameters. In our research, based on a statistical method (value of Fisher coefficient, *F*), textural entropy was selected and it turned out to be a satisfactory feature for the radiograph analysis. The proposed texture evaluation parameter increases in the radiographic region of interest, which indicates that during the healing process the bone becomes more and more complex in its structure.

Entropy is a measure of structure disarrangement. We assumed that it attains minimal values in a bone loss region which is structurally homogeneous. In the course of the bone healing process, when heterogeneity in optical density (complicated new bone elements) appears, the entropy value should increase, achieving a maximum level in a healthy or a totally regenerated trabecular bone tissue. In our study we found that the mean value of the evaluated parameter is significantly decreased in the bone defect region as compared to the reference bone. In the course of the healing process, it increases to reach the reference value, regardless of the gender and location. Furthermore, the pattern of the parameter change was similar in every analyzed group: in males and females, and in both locations – the maxilla and the mandible (Table II). This evidences that entropy may be use-

Table II. Summary statistics of texture parameter entropy

Group	*N*	Average	Median	Standard deviation	Minimum	Maximum	Range	Standard skewness	Standard kurtosis
T0_F_max_DEF	10	2.54	2.61	0.26	2.02	2.8	0.78	–1.21	0.06
T1_F_max_DEF	10	2.65	2.66	0.15	2.47	2.89	0.42	0.16	–0.6
T2_F_max_DEF	10	2.72	2.75	0.16	2.42	2.92	0.49	–1.03	–0.06
T0_F_max_REF	10	2.79	2.81	0.11	2.55	2.9	0.35	–1.49	0.95
T1_F_max_REF	10	2.78	2.91	0.18	2.54	2.93	0.39	–0.68	–1.37
T2_F_max_REF	10	2.79	2.78	0.12	2.54	2.97	0.44	–1.1	1.46
T0_F_man_DEF	10	2.54	2.57	0.21	2.16	2.82	0.66	–0.73	–0.17
T1_F_man_DEF	10	2.62	2.62	0.19	2.3	2.91	0.62	–0.25	–0.35
T2_F_man_DEF	10	2.69	2.7	0.21	2.38	3.02	0.64	–0.01	–0.35
T0_F_man_REF	10	2.85	2.88	0.13	2.54	2.96	0.42	–2.37*	2.53*
T1_F_man_REF	10	2.81	2.79	0.1	2.65	2.98	0.34	0.53	–0.15
T2_F_man_REF	10	2.69	2.67	0.17	2.43	2.95	0.52	0.24	–0.34
T0_M_max_DEF	10	2.49	2.56	0.24	2.08	2.81	0.72	–0.9	–0.38
T1_M_max_DEF	10	2.65	2.65	0.19	2.29	2.94	0.65	–0.49	–0.1
T2_M_max_DEF	10	2.84	2.91	0.17	2.55	3.01	0.47	–0.89	–0.75
T0_M_max_REF	10	2.84	2.91	0.18	2.46	3.01	0.56	–1.54	0.31
T1_M_max_REF	10	2.79	2.8	0.14	2.57	2.98	0.41	–0.56	–0.54
T2_M_max_REF	10	2.8	2.9	0.2	2.51	3.0	0.49	–0.88	–1.0
T0_M_man_DEF	10	2.47	2.49	0.28	2.05	2.88	0.83	–0.06	–0.83
T1_M_man_DEF	10	2.81	2.84	0.12	2.54	2.92	0.38	–1.98	1.2
T2_M_man_DEF	10	2.86	2.93	0.18	2.47	3.06	0.59	–1.60	0.76
T0_M_man_REF	10	2.87	2.93	0.18	2.41	3.05	0.65	–2.81*	3.59*
T1_M_man_REF	10	2.96	2.99	0.07	2.83	3.01	0.18	–1.52	–0.06
T2_M_man_REF	10	2.88	2.93	0.18	2.48	3.05	0.56	–1.94	1.03

**Lack of normal distribution. Max – maxilla, man – mandible, DEF – bone defect, REF – reference bone*

ful as a universal bone regeneration assessment feature.

The common radiological method of bone assessment presented in the literature is dual-energy X-ray absorptiometry (DXA). It allows one to assess bone mineral density (BMD), but without distinguishing the bone structure. For this reason, it is only exceptionally used in maxillofacial surgery. Ranjanomennahary *et al.* compared bone mineral density with two-dimensional textural features extracted from digital radiographs to three-dimensional microarchitecture of trabecular bone [13]. They confirmed that the use of co-occurrence matrix derived parameters enables one to extract precise information about three-dimensional structure from two-dimensional radiographs.

Widespread two-dimensional X-ray radiographs are sufficient for three-dimensional bone architecture assessment [14, 15]. This relevance is revealed in a large variety of texture analyses [16]. In a mathematical model of bone texture parameter analysis neither radiograph exposure conditions nor the size of the tagged region of interest should be taken into consideration, assuming that in the analyzed region (ROI) no tissues other than the bone appear [17, 18]. Computer assisted analysis demands setting of comparable features and methods. There is still no single universal method for bone structure assessment. Saparin *et al.* developed a nondestructive and noninvasive method for numeric characterization of the structural composition of human bone tissue [19]. Strong correlations were established between the measures of complexity and histomorphometric parameters. Carballido-Gamio *et al.* used fuzzy logic to assess trabecular bone quality with high-resolution magnetic resonance imaging (HR-MRI) [20]. Measures of fuzziness showed consistent correlations with trabecular number parameters, suggesting that the level of fuzziness could be related to the trabecular bone structure. Thus, it seems suitable to look for the entropy of the texture as a proper parameter for bone structure assessment. Rocha *et al.* evaluated new bone matrix formation by image texture analysis determining entropy and the fractal dimension of digital images [21]. They assessed bone regeneration in relation to the healing time and in comparison to images captured from the neighboring original bone structure. According to the authors, the presence of lamellar bone and formation of osteons gives an account of the stage of progression of bone remodeling and could be evaluated using the entropy of information and the fractal dimension of the new-formed bone. This method is similar to the one used in our study.

In conclusion, on the basis of computer assisted radiological research, textural entropy proved to be a potential parameter to assess regeneration of bone tissue. The calculated parameter in the investigated material revealed a gradual decrease of simplicity of the texture inside the bone defect in time, up to the most complex structure one year postoperationally, reaching the reference bone level. Moreover, entropy relevance to the bone structure and the study methodology could be easily applied in other radiological examination methods, i.e. computed tomography and cone-beam computed tomography, due to similarity of source data.

Acknowledgments

The study was supported by the Medical University of Lodz, grant no. 502-03/5-138-03/502-54-083.

References

1. Fili S, Karalaki M, Schaller B. Therapeutic implications of osteoprotegerin. Cancer Cell Int 2009; 9: 26-33.
2. Baczyk G, Opala T, Kleka P, Chuchracki M. Multifactorial analysis of risk factors for reduced bone mineral density among postmenopausal woman. Arch Med Sci 2012; 8: 332-41.
3. Li J, Wang X, Zhou C, et al. Perioperative glucocorticosteroid treatment delays early healing of a mandible wound by inhibiting osteogenic differentiation. Injury 2012; 8: 1284-9.
4. Moya-Villaescusa MJ, Sánchez-Pérez A. Measurement of ridge alterations following tooth removal: a radiographic study in humans. Clin Oral Impl Res 2010; 2: 237-42.
5. Eickholz P, Krigar DM, Kim TS, Reitmeir P, Rawlinson A. Stability of clinical and radiographic results after guided tissue regeneration in infrabony defects. J Periodontol 2007; 78: 37-46.
6. Rosa GM, Lucas GQ, Lucas ON. Cigarette smoking and alveolar bone in young adults: a study using digitized radiographs. J Periodontol 2008; 79: 232-44.
7. de Oliveira R, Macedo G, Muglia V, Souza S, Novaes A, Taba M. Replacement of hopeless retained primary teeth by immediate dental implants: a case report. Int J Oral Maxillofac Implants 2009; 24: 151-4.
8. Benhamou CL, Poupon S, Lespessailles E, et al. Fractal analysis of radiographic trabecular bone texture and bone mineral density: two complementary parameters related to osteoporotic fractures. J Bone Miner Res 2001; 16: 697-704.
9. Lespessailles E, Gadois C, Kousignian I, et al. Clinical interest of bone texture analysis in osteoporosis: a case control multicenter study. Osteoporos Int 2008; 19: 1019-28.
10. Chai HY, Wee LK, Swee TT, Saleh ShH, Chea LY. An artifacts removal post-processing for epiphyseal region-of-interest (EROI) localization in automated bone age assessment (BAA). Biomed Eng Online 2011; 10: 87.
11. Szczypiński PM, Strzelecki M, Materka A, Klepaczko A. MaZda – a software package for image texture analysis. Comput Methods Programs Biomed 2009; 94: 66-76.
12. Schürman J. Pattern classification. John Wiley & Sons, New York 1996.
13. Ranjanomennahary P, Ghalila SS, Malouche D, et al. Comparison of radiograph-based texture analysisand bone mineral density with three-dimensional microarchitecture of trabecular bone. Med Phys 2011; 38: 420-8.
14. Luo G, Kinney JH, Kaufman JJ, Haupt D, Chiabrera A, Siffert RS. Relationship between plain radiographic

patterns and three- dimensional trabecular architecture in the human calcaneus. Osteoporos Int 1999; 9: 339-45.
15. Pothuaud L, Benhamou CL, Porion P, Lespessailles E, Harba R, Levitz P. Fractal dimension of trabecular bone projection texture is related to three-dimensional micro-architecture. J Bone Miner Res 2000; 15: 691-9.
16. Apostol L, Boudousq V, Basset O, et al. Relevance of 2D radiographic texture analysis for the assessment of 3D bone microarchitecture. Med Phys 2006; 33: 3546-56.
17. Shrout MK, Potter BJ, Hildebolt CF. The effect of image variations on fractal dimension calculations. Oral Surg Oral Med Oral Pathol Oral Radiol Endod 1997; 84: 96-100.
18. Shrout MK, Hildebolt CF, Potter BJ. The effect of varying the region of interest on calculations of fractal index. Dentomaxillofac Radiol 1997; 26: 295-8.
19. Saparin P, Thomsen JS, Kurths J, Beller G, Gowin W. Segmentation of bone CT images and assessment of bone structure using measures of complexity. Med Phys 2006; 33: 3857-73.
20. Carballido-Gamio J, Phan C, Link TM, Majumdar S. Characterization of trabecular bone structure from high-resolution magnetic resonance images using fuzzy logic. Magnetic Resonance Imaging 2006; 24: 1023-9.
21. Rocha LB, Adam RL, Leite NJ, Metze K, Rossi MA. Bio-mineralization of polyanionic collagen-elastin matrices during cavarial bone repair. J Biomed Mater Res Part A 2006; 79: 237-45.